

Chapter 3

On the study areas

The 7500 km mountain chain of the Andes forms the western margin of the South American continent, where oceanic plate material of presently two plate segments (Nazca and Antarctic plate) is being subducted beneath the continental lithosphere (figure 3.1). Since plate convergence is known to have occurred there at least since Jurassic time, the Andes have been considered an exemplary model of a subduction orogen. However, subducting/ed ocean ridges, frequent changes in convergence rate and direction, and several terranes that are discussed to have accreted to the continental margin before Jurassic time (*Mpodozis C.* [1990], *Gallagher* [1990]) give the western margin of the South American continent a complex history. In and before Cambrium (~500 Ma), the eastern part of the present North American continent ('Laurentia') is discussed to have been adjacent to the Central and Southern Andes (*Gallagher* [1990]).

Volcanism along the Andes can be divided into the northern (2°S–5°S), central (16°S–28°S) and southern (31°S–52°S) zones and is confined to areas with sufficiently steep dip of the subducted plate (*Cahill and Isacks* [1992], *Chen et al.* [2001]).

3.1 The Central Andes

Altiplano-Puna plateau

Between 16°S and 25°S latitude, the subduction orogen of the Andes widens enormously, comprising in its center the 1800 km long and 350–400 km wide Altiplano-Puna plateau with average elevations of 3500–4500 m and an 250–300 km wide area of internal drainage, thus being the in height and extent largest non-collisional plateau on earth (*Isacks* [1988]). The topography of this mountain chain, as well as that of the underlying Wadati-Benioff zone, exhibits a high degree of symmetry around the so-called Arica bend, and the north pole of the corresponding symmetry axis coincides roughly with the Tertiary rotation poles and the orientation of the actual Nazca/South America Euler vector (*Gephart* [1998]). The Central Volcanic Zone, with holocene volcanism mainly in the Western Cordillera, is confined to the mid Central Andes, where subduction is comparably steep (~30° at 100 km depth). North and south of this zone, subduction shallows significantly and no Post-Pliocene volcanism is documented (*Isacks* [1988]).

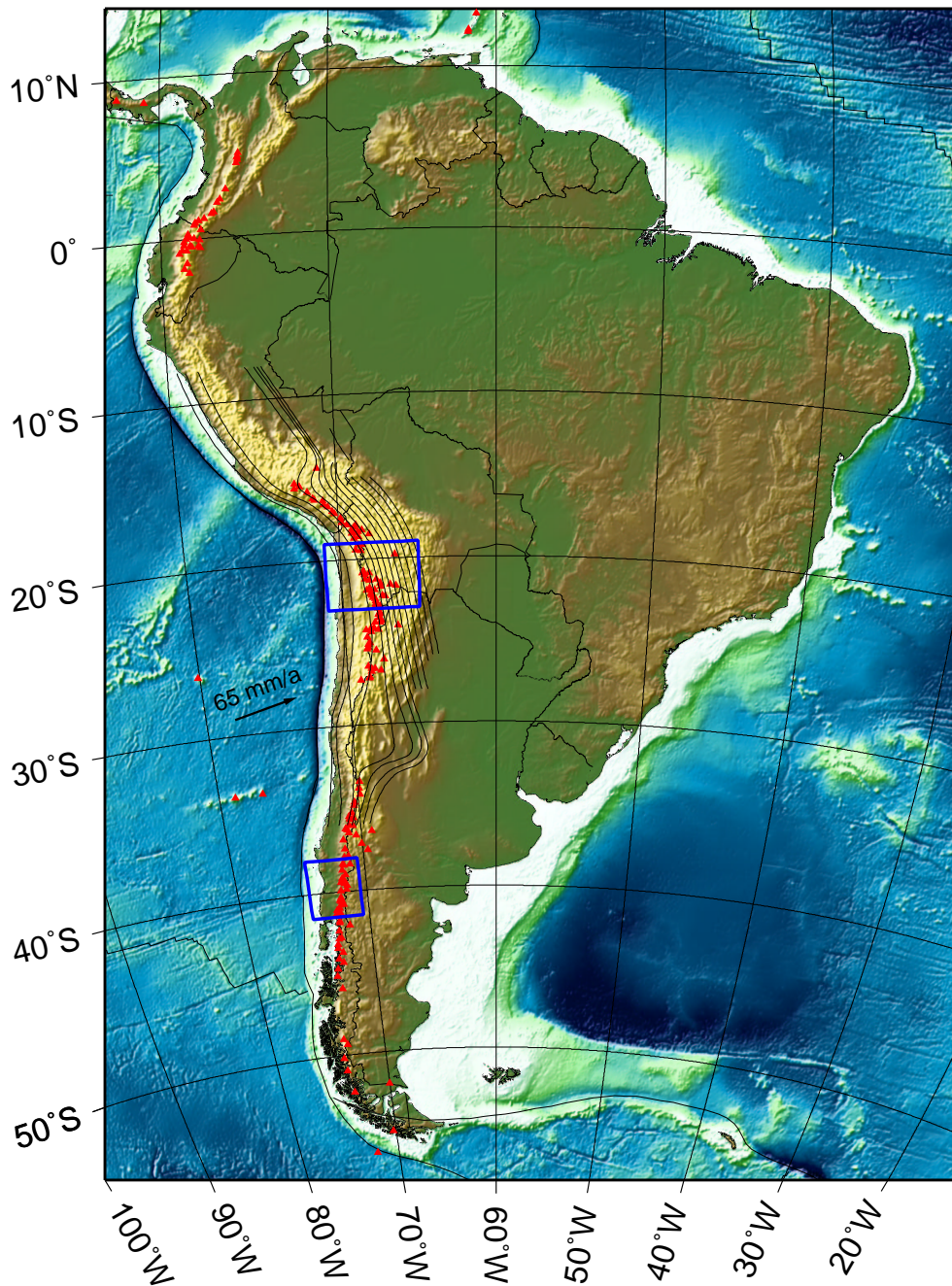


Figure 3.1: Topography and bathymetry around South America (data from Smith and Sandwell [1997]). Depth isolines (from left: 50 km to right: 350 km with 25 km intervals) of hypocenter locations from globally registered earthquakes illustrate the shape of the Wadati-Benioff zone between 8°S and 36°S (from Isacks [1988]). The oceanic Nazca plate converges with the continental South American plate at a rate of 65 mm/a and an angle of N77°E (Angermann and Reigber [1999]). Holocene volcanoes are marked by red triangles (catalogue from Smithsonian Institution, Global Volcanism Program). Rectangles indicate the location of the two magnetotelluric study areas at ~21°S (campaigns in 1993-1998) and ~39°S (2000).

3.1 THE CENTRAL ANDES

Below the Western Cordillera and the Altiplano, the crust is thickened to approximately 70 km (*James* [1971], *Götze et al.* [1994], *Wigger et al.* [1994], *Beck et al.* [1996], see also below). Crustal shortening is supposed to account for the most part of the thickening, and to what extent magmatic addition and tectonic underplating additionally contribute is still being debated (*Allmendinger et al.* [1997]). Shortening, thus obviously timing the uplift, occurred in a principal phase from about 25 Ma to 10 Ma, when the trench-normal convergence rate increased markedly and volcanism, before that area confined to the west, spread eastward across the Altiplano. After ~ 9 Ma, deformation was shifted eastward to the Subandean Belt, still contributing to crustal thickening (*Isacks* [1988], *Allmendinger et al.* [1997]).

Magmatic and tectonic history

The formation of all major morphological units within the study area, that today exhibits an arid to semiarid climate, is directly related to the history of arc magmatism of the Andean orogenic cycle since Liassic time, during which magmatic activity several time shifted eastwards, obviously due to ongoing tectonic erosion at the leading edge of the overriding South American continent (*Coira et al.* [1982]). The following description of these units is mainly taken from *Scheuber and Reutter* [1992].

In Jurassic to Early Cretaceous time, the magmatic arc was situated in the actually ~ 2000 m high Coastal Cordillera, where in an orogen-normal extensional regime lavas erupted in a shallow marine basin, and large plutons and dykes intruded into a continental basement. This zone exhibits the along more than 1000 km ($20^{\circ}\text{S} - 30^{\circ}\text{S}$) tracable orogen-parallel Atacama Fault zone (see figure 3.2). Main movements within this zone, due to its relationship with intrusions, can be dated to the same age as magmatism. The uniformly sinistral orientation of strike-slip faults within the system fits well with the reconstruction of a sinistral convergence between the South American Plate and the oceanic 'Aluk' plate (*Zonenshayn et al.* [1984], similar as figure 3.3 right). In mid-Cretaceous time, the volcanic arc was located further to the east where is now the Longitudinal Valley (~ 1000 m above sea level). In the end of this phase, strong deformations have occurred in a compressional regime, an observation which is in accordance with a change in the configuration of the oceanic plates, leading to dextral convergence of smaller obliqueness (figure 3.3). In the actual Precordillera, which reaches elevations > 5000 m above sea level, the volcanic arc was located from latest Cretaceous to Oligocene, and to the east of it a large extensional backarc basin developed in this time, with marine ingression, strong sedimentation and also magmatism. The Precordillera comprises signatures of strong folding and faulting, involving basement rocks that appear in the core of broad anticlines (*Isacks* [1988] proposed the Precordillera to be a crustal-scale monocline, tracking the tip of an asthenospheric wedge below the orogen). This area exhibits the orogen-parallel Precordillera Fault System (including the West Fissure, see figure 3.2), comprising mainly dextral strike-slip movement, which is in general accordance with still dextral plate convergence in this era. Here too the time span of strong deformation in Late Eocene and Early Oligocene, involving the formation of a fold and thrust belt in the backarc up to the actual Eastern Cordillera, coincides with an increased convergence rate between the Farallon/Nazca plate and the continent.

Since Miocene, the magmatic arc is emplaced in the Western Cordillera (with the highest peaks exceeding 6000 m altitude), upon the backarc fold and thrust belt of the preceding arc.

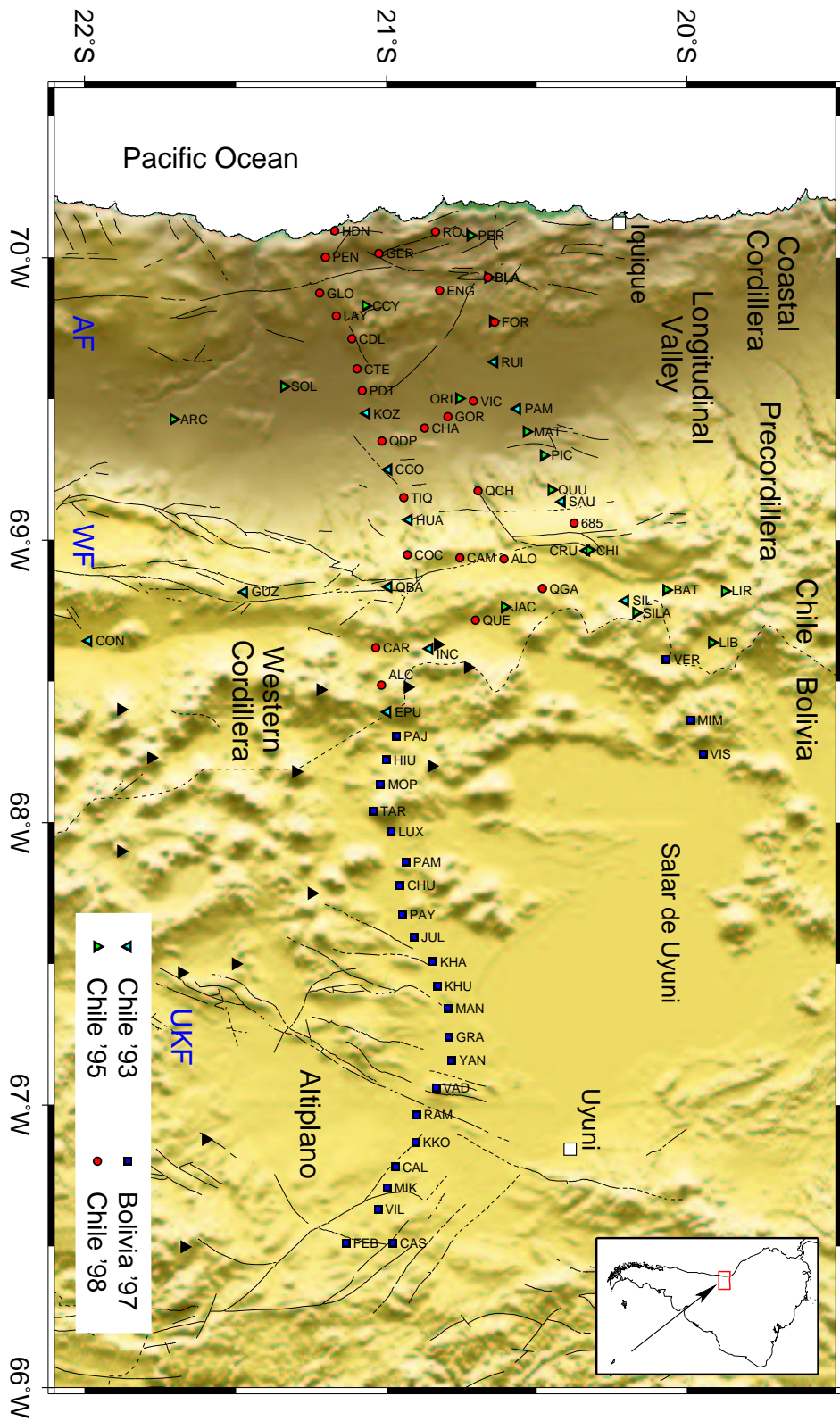


Figure 3.2: Site locations from four long period magnetotelluric campaigns in the southern Central Andes. Most sites are aligned along profiles: the northern PICA (210 km, ~16 stations) and the southern ANCORP profile (370 km, 38 stations) at ~21°S. Compiled fault data from Reutter et al. [1994] show the major fault zones traversing the study area: The coast-parallel Atacama fault (AF), the Precordillera fault zone including the West Fissure (WF), and the NNE oriented Uyuni-Kenyani Fault in the Altiplano. Black triangles mark holocene volcanoes.

3.1 THE CENTRAL ANDES

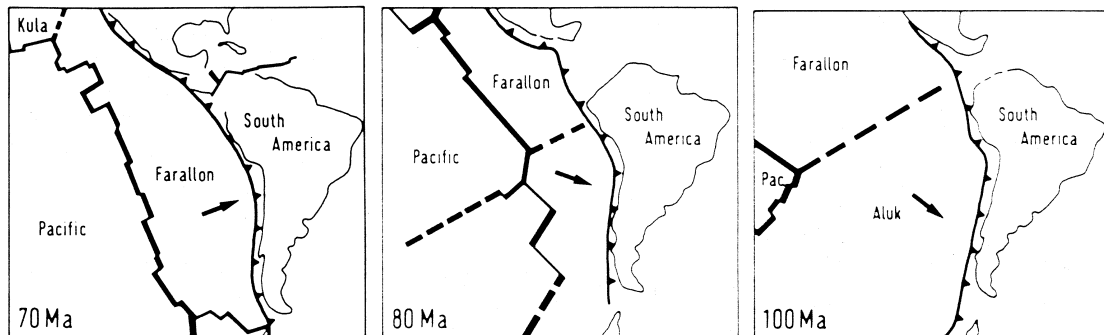


Figure 3.3: Reconstruction of plate configurations in the Southeast Pacific between 100 Ma and 70 Ma (from Scheuber and Reutter [1992]). The reorganization led to a reduced obliqueness of convergence and correlates temporally with enhanced deformation in the Central Andes.

Though activity concentrates in the West, volcanism is observed up to the western part of the Eastern Cordillera, often aligned along fracture systems, which points out the linking between tectonics and magmatism. The actual trench is about 100 km offshore and up to 8000 m deep, almost free of sediments, and debris at the base of the continental slope is underthrust with the subducting plate (von Huene *et al.* [1999]).

Previous electromagnetic studies

First magneto-variational studies in the Central Andes were carried out by U. Schmucker in 1962 and 1965 in Peru and central-western Bolivia. Analyzing so-called bay events of about two hours' duration, Schmucker *et al.* [1966] calculated vectors of horizontal geomagnetic perturbation and anomalous tipper functions of together 12 field stations (see figure 3.4), which could be reproduced by modelling a deep high conductivity anomaly below the crust under the western limit of the Eastern Cordillera.

Between 1982 and 1989, the Berlin research group "Mobility of Active Continental Margins" — the predecessor of the SFB267 — within seven field campaigns carried out long period electromagnetic measurements, deploying altogether 120 field stations between 21°S and 25°S in northern Chile, southern Bolivia and northwestern Argentina. From these data, by successive forward modelling adjusting longitudinal and transverse impedances as well as geomagnetic transfer functions, Krüger [1994] developed three 2-D conductivity models of adjacent regions, which were combined to one Andean resistivity cross section, running *representatively* along 21.45°S from the Pacific coast to the Chaco lowlands east of the Eastern Cordillera (Schwarz and Krüger [1997]). The western profile crosses the Western Cordillera at 22.5°S. Below the Coastal Cordillera and the Longitudinal Valley, the model comprises vertical dike-like conductors, which macroscopically account for proposed anisotropy. While the subsurface of the Precordillera is modelled resistive, a large zone of anomalous high conductivity ($< 2 \Omega\text{m}$) was deduced below the Western Cordillera and the Altiplano, with highest conductances (depth-integrated conductivities) below the Western Cordillera ($> 23,000 \text{ S}$), and toward the eastern Altiplano with again increasing conductances. On top of the Altiplano, a conductive sedimentary cover was modelled with highest conductances again in the eastern Altiplano. Eastward of the Eastern Cordillera, conductivities are strongly decreased,

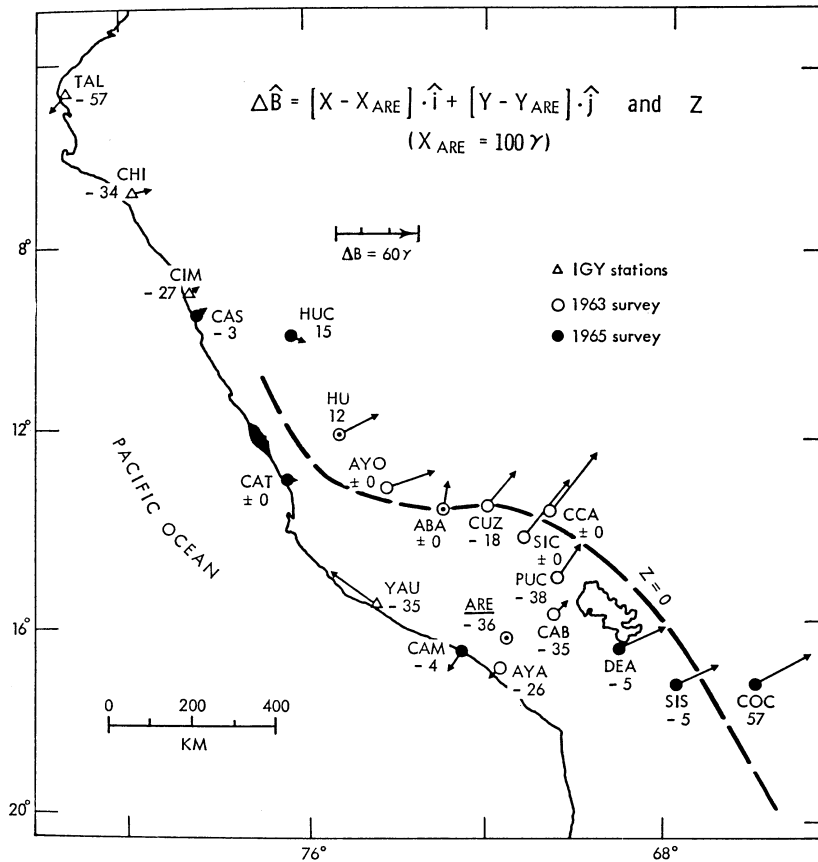


Figure 3.4: The Andean anomaly after Schmucker *et al.* [1966], deduced from simultaneously recorded bay-events, which's normal geomagnetic field is oriented mainly N-S. The line of zero B_z variation marks the lateral trend of the anomaly, and 'perturbation vectors', representing the anomalous horizontal magnetic field (corresponding to $\mathbf{p} = h_H \hat{\mathbf{x}} + d_H \hat{\mathbf{y}}$, cf. equation 2.15) are properly oriented perpendicular to this line. Numbers refer to amplitudes of the vertical magnetic field component.

except for small-scale conductive structures in the upper crust of the Subandean Ranges and the Chaco, simulating again anisotropy.

Analyzing data which are also reexamined in this study, *Echternacht et al.* [1997] (see also *Echternacht* [1998]) by successive forward modelling of impedance data and geomagnetic transfer functions derived a 2-D model for the Chilean part of the PICA profile ($\sim 20.5^\circ\text{S}$), thus reaching from the Pacific coast to the Western Cordillera. His results contrast sharply those of *Krüger* [1994] and *Massow* [1994] from the study area located roughly 200 km further south: The model exhibits no deep conductivity anomaly below the Western Cordillera, and also under both the Coastal Cordillera and the Longitudinal Valley, no deep conductors are inferred. Instead, a high conductive zone ($\sim 2\Omega\text{m}$) below the Precordillera is modelled between 8 km and 25 km depth, and under this anomaly a second anomaly extends from 80 km to 180 km depth, which for the most part would actually be situated below the subducting Nazca plate.

3.1 THE CENTRAL ANDES

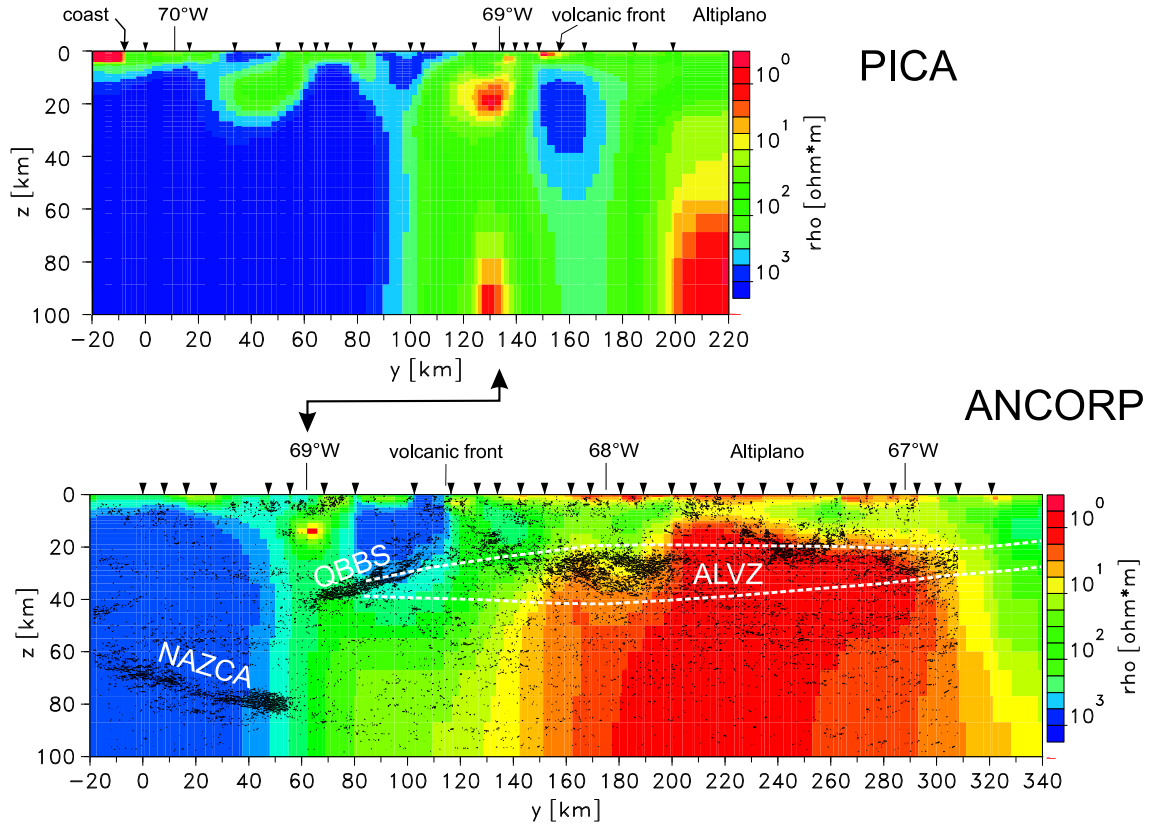


Figure 3.5: Results from bimodal impedance inversions for the PICA and ANCORP profiles (Brasse et al. [2002]). Superimposed on the conductivity model of the latter profile are the Andean low velocity zone (ALVZ), derived from receiver function analysis (Yuan et al. [2000]), and line drawings from seismic reflection analysis (redrawn from M. Stiller, pers. comm.). ‘QBBS’ (Quebrada Blanca bright spot) marks a highly reflective zone between the Precordillera and the Western Cordillera. In both inversions, the Pacific ocean was included as a-priori information.

Schwalenberg [2000] (see also Brasse et al. [2002]) derived a two-dimensional conductivity model from impedance data of 33 stations of the ANCORP profile ($\sim 21^\circ\text{S}$), inverting for impedance data of both modes (figure 3.5). The modelled part of the profile extends from the Longitudinal Valley (CTE) to the foothills of the Eastern Cordillera (CAS). In accordance with Echternacht et al. [1997], the model comprises high resistivities below the Coastal Cordillera and the Longitudinal Valley, and also below the Western Cordillera, no conductor is postulated. Like further north, a high conductivity anomaly of small lateral and vertical extent has been found beneath the Precordillera in ~ 20 km depth (the second, deeper anomaly is missing). Under the Altiplano, which is covered by highly conductive sediments (first kilometers), below ~ 20 km depth, a huge anomaly of conductivities ($\lesssim 1 \Omega\text{m}$) is modelled, which’s lower boundary is not resolved, respectively the model exhibits no lower boundary. Having applied various 2-D resolution studies, Schwalenberg [2000] concluded that the anomaly should extend at least to 60 km depth. With the same technique, Brasse et al. [2002] reexamined the data from the PICA profile, now including three more stations located in Bolivia. The model, comprising a Precordillera anomaly which is more significant than at 21°S , basically reproduces the conductivity distribution deduced by Echternacht et al. [1997], but

on account of the additional stations now at its eastern margin indicates a high conductivity anomaly below the Altiplano, as found further south (figure 3.5).

Lezaeta [2001] developed a 3-D model for the eastern part of the study area from the coast up to the Western Cordillera, analyzing data from both profiles and in between. The model, which amongst others is composed of 2-D bimodal impedance inversion results, 3-D thin sheet forward modelling studies for the Precordillera and 3-D modelling studies for the coastal region, explains to a certain extent both, impedance and geomagnetic data. The Atacama Fault Zone in the Coastal Cordillera, where strong distortion effects are observed (see section 5.1 and *Lezaeta* [2001]), is modelled as a combined system of confined dykes of unknown vertical extent. Below the Precordillera, separate conductivity anomalies are postulated in different depth ranges: The upper one, which mainly accounts for observed geomagnetic transfer functions, is in ~ 5 km depth and comprises one branch in northwestern direction. The deeper anomaly between 10 and 30 km depth, as suggested by 2-D inversion models mentioned above, has highest conductivities in the north, and conductivities decrease gradually towards south. This, together with a westward bending of the Altiplano conductor in the north, *partially* reproduces south components of induction vectors as they are observed in the Precordillera and the Preandean Depression.

In the study in hand, data from long period electromagnetic recordings of all stations in figure 3.2 (i.e. PICA and ANCORP profiles plus stations in between) are reinvestigated in the sense of a geomagnetic array data analysis, taking advantage of the partly simultaneous nature of the data.

Other geophysical observations

From a seismic reflection experiment along the ANCORP line, a zone of high reflectivity could be imaged on top of the subducting Nazca plate between 40 and 80 km depth, its deeper bound located roughly 20 km above a cluster of intermediate-depth earthquakes, indicating that these earthquakes occur within the oceanic upper mantle and that the Wadati-Benioff zone does therefore not image the crust of the subducting plate (*ANCORP Working Group* [1999])¹. Beneath the western limit of the Western Cordillera, in 20 km depth the highly reflective ‘Quebrada Blanca bright spot’ is observed, dipping west and extending to the west below the Precordillera, where it ends in 35 km depth. This feature is regarded as an image of rising fluids, but electromagnetic data do not support this assumption (*Schwalenberg* [2000], *Brasse et al.* [2002]). The area beneath the Western Cordillera does not reveal enhanced reflectivity, whereas below the Altiplano, two centers of diffuse reflectivity were found, with thicknesses of 10–15 km, their upper bounds being in ~ 20 km (west) and ~ 15 km (east) depth, respectively (see figure 3.5). Wide-angle reflection analysis of the same data set revealed low P wave velocities (3.8–5.8 km/s) down to 15 km under the Altiplano, and – not well resolved – a 10 km thick layer beneath with lowest velocities in the eastern Altiplano (5.7–6.2 km/s, *Lüth* [2000]). A velocity contrast in ~ 20 km depth in the forearc is interpreted as a ‘Paleo-Moho’, the base of the Jurassic crust. From a seismic refraction experiment along the same

¹A reanalysis of this data by *Yoon* [2001] could image the Nazca reflector to slightly greater depths. *Yoon* [2001] proposes a due to hydration processes altered zone above the subducting plate to account for the reflections, still assuming that the earthquakes below occur in the oceanic lithosphere.

3.1 THE CENTRAL ANDES

line, no signals from deep structures were obtained on the Altiplano, indicating a weakened crust with reduced velocities (*Wigger et al.* [1994]).

Beck et al. [1996] derived crustal thicknesses for the Central Andes with receiver function analysis of seismic broadband data from intermediate to deep earthquakes within the subducting Nazca plate as well as from teleseismic earthquakes, recorded in the BANJO and SEDA experiments north of 21.5°S. Maximal thickness is found below the Western Cordillera with 70–74 km, and Altiplano crustal thickness ranges from 60 to 65 km, with slight increase towards the Eastern Cordillera, before it drops down to ~45 km beneath the Subandean Ranges (all at 20°S). Modelling wave forms from the regional sources, *Zandt et al.* [1996]² and *Swenson et al.* [2000] estimated average crustal P velocities of 6.0 km/s and a Poisson ratio of 0.25 (for the mantle below: 0.27–0.29), concluding that the Altiplano crust has to be quartz-rich and felsic, and therefore proposing that tectonic shortening without significant magmatic addition due to intrusions from the mantle accounts for the thickening of the crust. *Baumont et al.* [1999] observed strong attenuation of crustal seismic *Lg* and *Pg* phases from regional earthquakes at crustal depths, recorded at stations of the same experiments including those of the ‘Lithoscope’ networks. Since most of the attenuation was found to be frequency independent, the authors favor scattering rather than intrinsic attenuation (which for *Lg* was estimated to ≈ 200) to account for the observation, and, referring to *O’Connell and Budiansky* [1977], exclude a percentage of partial melt higher than 1%, which is in accordance with the Poisson number of 0.25 (figure 3.6).

Haberland and Rietbrock [2001] derived a 3-D (Q_p^{-1}) attenuation model³ from data of local earthquakes from the Wadati Benioff zone recorded at the PISCO and ANCORP seismic networks. Strongest attenuation ($Q_p < 100$) is found in 15 km to 55 km depth beneath the Western Cordillera between 22°S and 23°S, which is in very good correlation with the electromagnetic observation of a high conductivity zone beneath the volcanic arc at 22.5°S and the missing of such zone at 21°S and 20.5°S (figure 3.7; the Altiplano is not included in this modelling). Using seismic data from several networks, *Yuan et al.* [2000] deduced a 10–20 km thick low velocity zone below the entire Altiplano, averaging over 4 degrees of latitude from 20°S to 24°S (for the location of this layer, see figure 3.5). Also by receiver function analysis, *Chmielowski et al.* [1999] proposed a <1 km thick layer of extremely low shear wave velocity (<0.5 km/s) in ~19 km depth, extending throughout the Altiplano Puna Volcanic Complex (APVC, *de Silva* [1989]), which reaches from 21°S to 24°S.

Measured heat flow densities in the Western Cordillera and the Altiplano exceed 100 mW/m² (*Henry and Pollack* [1988]). *Springer* [1999] derived a 2-D model from a compilation of heat flow data along 21°S. This modelling, which yields a high temperature gradient beneath the Western Cordillera and the Altiplano (the 600°C isotherm is in 40 km depth) includes an asthenospheric mantle wedge reaching to the west at least below the Western Cordillera. Calculated heat flow densities on the Altiplano are lower than the measured average — locally high heat flow values are supposed to be on account of isolated, short-lived magma chambers.

²Their 1-D model has an upper layer of 10 km with $v_p = 5$ km/s, followed by a 47 km layer of $v_p = 6.2$ km/s and an 8 km transition zone of $v_p = 7$ km/s. Below the Moho, P wave velocity is modelled with 8.1 km/s.

³P wave velocity was assumed to be frequency independent in this modelling.

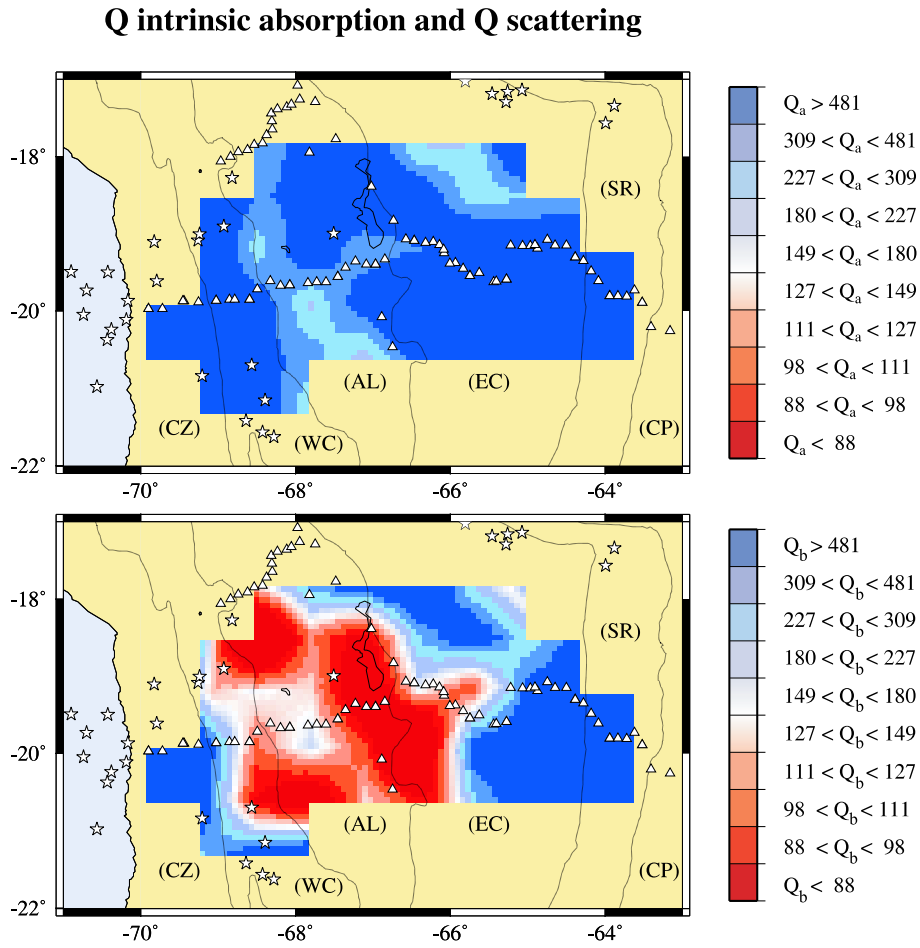


Figure 3.6: Apparent attenuation of seismic Lg phases from regional crustal earthquakes, recorded in the BANJO, SEDA and Lithoscope experiments (from Baumont *et al.* [1999]). Plotted are the results Q_a (top) and Q_b (bottom) of a parametric analysis for a functional dependence $Q_s^{-1}(f) = Q_a^{-1} + (Q_b f)^{-1}$ for the period range [1–5 Hz]. Most of the measured attenuation Q_s^{-1} is frequency dependent and therefore supposed to be due to scattering.

Beck *et al.* [1996] (see above) compared crustal thicknesses obtained by receiver function analysis with from topography data estimated crustal roots, assuming isostatic compensation (with constant crustal and mantle densities of 2.7 g/cm^3 and 3.3 g/cm^3 , respectively). Since the thicknesses roughly coincide, the authors conclude that the Central Andes are at first order in Airy-type isostatic equilibrium. Gravity data reveal a strong Bouguer anomaly, with a minimum of about -450 mGal in the Altiplano. More sophisticated gravimetric modelling based on detailed seismic velocity data and using velocity-density relationships, for the most part reproduces the measured Bouguer anomaly (Götze and Kirchner [1997]). Significant positive isostatic residuals remain in the Coastal Cordillera ($\sim 70 \text{ mGal}$), in the eastern part of the Eastern Cordillera ($< 40 \text{ mGal}$) and in the central Altiplano ($< 30 \text{ mGal}$); The Western Cordillera and the western part of the Eastern Cordillera reveal negative residuals (40 mGal and 20 mGal , respectively).

3.2 THE SOUTHERN ANDES

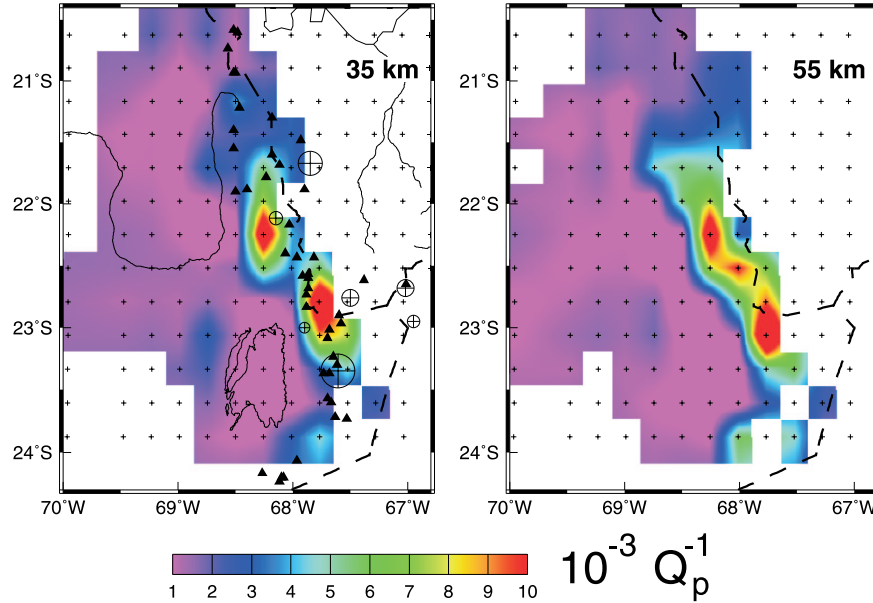


Figure 3.7: Slices at 35 km and 55 km depth through the 3-D (Q_p^{-1}) attenuation model from Haberland and Rietbrock [2001], obtained from local earthquake data, recorded at the ANCORP and PISCO seismological networks. Triangles mark recent volcanoes, circles indicate centers of silicic magmatism.

3.2 The Southern Andes

Convergence in the Southern Andes around 39°S latitude occurs with roughly the same rate (66 mm/a, Angermann and Reigber [1999]) and obliqueness ($\sim 25^\circ$ with respect to the orthogonal, Jarrard [1986]) as in the Central Andes, and also the down-dip of the Wadati-Benioff zone below 50 km depth is of comparable steepness ($\sim 30^\circ$, Bohm *et al.* [2002]). Yet, the tectonic setting is very different to the south.

The trench is only < 4.5 km deep and, due to the humid climate in south Chile, filled with a ~ 1500 m pile of turbidites, which are frontally accreted, underthrust and underplated (Bangs and Cande [1997], Diaz-Naveas [1999]). As a consequence to the accretionary nature of subduction, the volcanic arc did not move eastward as in the Central Andes, but remained relatively stationary from Jurassic to Quaternary in the Main Cordillera, where magmatic activity still takes place. This mountain chain, which's main axis is about 270 km off the trench, is only 70–120 km wide, and only highest peaks exceed 3000 m altitude, i.e. no plateau formation is observed in the Southern Andes. The Coastal Cordillera, with elevations < 1000 m, best exposes the metamorphic basement rocks which are the oldest rocks in this part of the Andes and are interpreted as part of a Late Paleozoic accretionary complex. This basement is intruded by a series of Late Triassic to Miocene plutons, the North Patagonian Batholith, which itself constitutes much of the basement of the Southern Andes (Pankhurst *et al.* [1992], Hervé *et al.* [1988]). Between 36°S and 39°S, the large Neuquén back arc basin developed during Jurassic to Early Cretaceous, which was filled with marine and continental deposits (Mpodozis *C.* [1990]). No fold and thrust belt developed east of the volcanic arc like in the Central Andes.

From the Chilean Ridge triple junction at 46°S up to 38°S , extending more than 950 km in length, the Liquiñe-Ofqui fault zone runs along the weakened zone of the Recent and Mio-Pliocene magmatic arc (*Cembrano et al.* [2000]). The fault divides an obviously due to oblique subduction (*Jarrard* [1986]) and especially in the south due to indentation of the Chile Ridge (*Nelson et al.* [1994]) relatively northward moving fore-arc from the South-American continent. Also the subducting oceanic plate aside the study area near 39°S is characterized by major fracture zones, most prominently the $\sim\text{N}60^{\circ}\text{E}$ running Mocha and the $\sim\text{N}80^{\circ}\text{E}$ oriented Valdivia fault. North of the former ($< 38^{\circ}\text{S}$), plate material was generated at the Pacific-Farallon spreading center at least 35 Ma ago, whereas south of the Valdivia fault, oceanic plate stems from the Chile Ridge and is younger than ~ 20 Ma. *Herron* [1981] noted that the main events of the great 1960 Valdivia earthquake (the strongest earthquake ever recorded) are located close to the continentward extension of the fault traces. Also, the intersection of the traces with the continental divide (which is the today's political border) marks right-lateral offsets of the latter, which for the Valdivia fault is just located north of 39°S . *Muñoz and Stern* [1988] reported a westward drift of the volcanic front from Pliocene-early Pleistocene to Quaternary between 38°S and 39°S , which is discussed to be in causal connection with the transform faults.

The only previous electromagnetic variation experiment in the region concerned was carried out in a collaboration project between Chile and Argentina in 1986 (*Muñoz et al.* [1990]). At nine field sites on a W-E profile running from near the coast to the Chilean/Argentinean border south of lake Villarrica ($\sim 39.3^{\circ}\text{S}$), impedance data were deduced from short (AMT) and long (MT) period equipment recordings (the latter partly analogue). One-dimensional and rough 2-D forward modelling (excluding the ocean) of shifted apparent resistivities revealed decreased resistivities below Villarrica volcano ($60\ \Omega\text{m}$), and a layer between 25 km and 45 km depth with from west toward east decreasing resistivities ($2000\ \Omega\text{m}$ to $100\ \Omega\text{m}$). In a reinvestigation of that data with still rough 2-D modelling now including the ocean, this layer has constant resistivity of $200\ \Omega\text{m}$ and rises towards east, and resistivities below Villarrica volcano decrease to $20\ \Omega\text{m}$ (*Muñoz et al.* [1992]).

In this study, data from together 34 long period magnetotelluric field stations (same equipment as deployed in the Central Andes), which recorded during a three-month period in late 2000, are analyzed with a focus on geomagnetic variations (figure 3.8). The sites are aligned along two profiles, a longer and denser one comprising 22 stations with a spacing of approximately 10 km, running from the Pacific coast (lake Budi) to the Chilean border with Argentina (east of the village Liucura) at 38.9°S , passing the volcanic arc just south of Llaima volcano, and a second shorter profile along 39.3° comprising 10 stations with wider spacing, which closely passes the Villarrica volcano at its northern flank and thus roughly matches the location of the pilot study of *Muñoz et al.* [1990]. Two additional stations were deployed 70 km and 140 km farther south to better constrain the geometry of observed higher subsurface dimensionality (section 8).

As a first concentrated seismic investigation of this area, the ISSA2000 experiment, with a seismic temporal network between 36°S & 40°S and 69°W & 76°W , and a refraction line along 39°S (i.e. the northern MT profile) was carried out in 2000 (*Bohm et al.* [2002]). Continuous seismicity within the Wadati-Benioff zone is observed to 120 km depth with concentrations

3.2 THE SOUTHERN ANDES

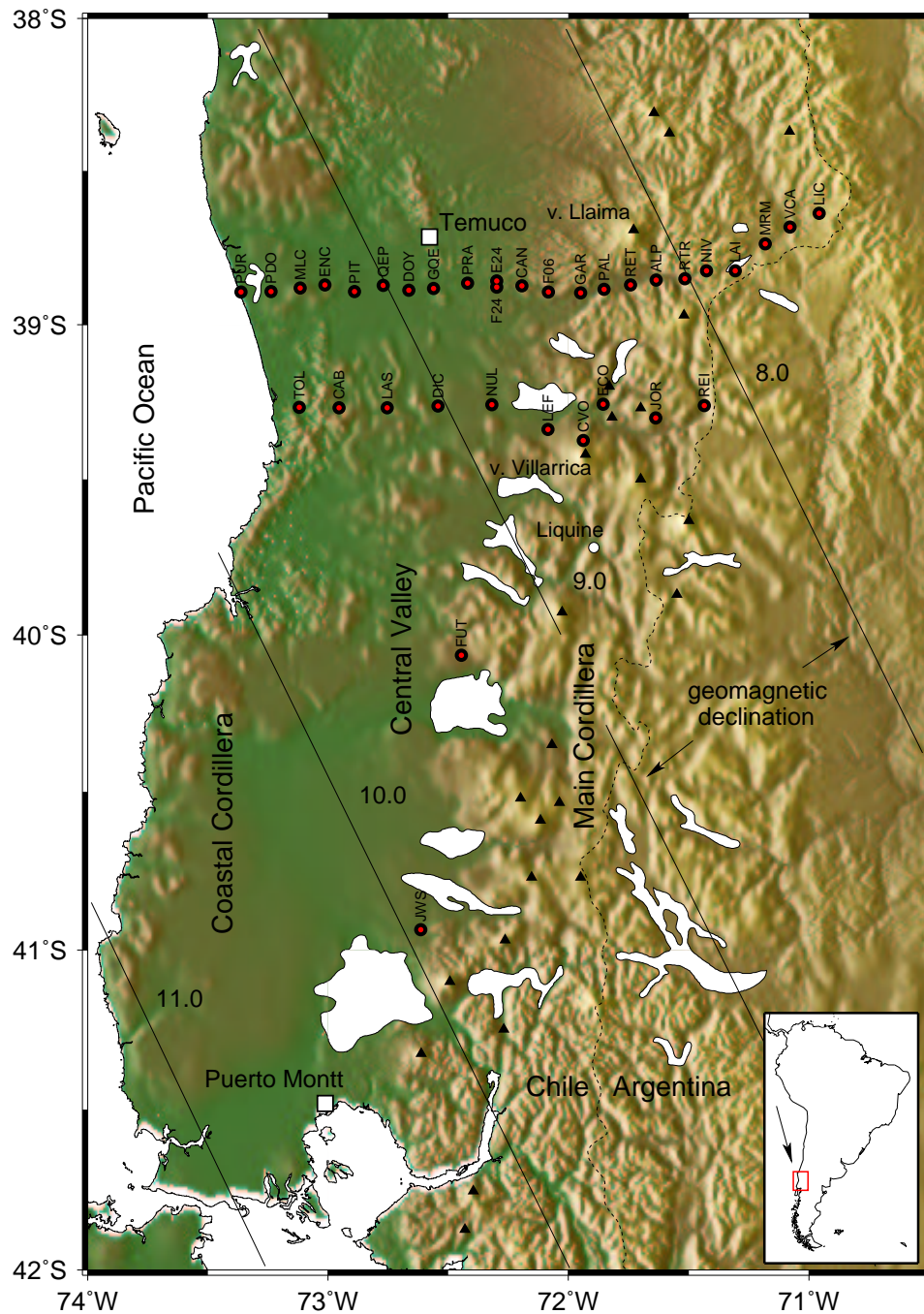


Figure 3.8: Study area and site locations from the 2000 campaign in the Southern Andes. Stations are aligned along two profiles. The main profile along $\sim 39^\circ\text{S}$ with a length of 210 km comprises 22 stations. Roughly 40 km further south, another 10 stations compose a second line, which is about 145 km long. The isolines of equal declination were calculated from International Geomagnetic Reference Field coefficients (IGRF 2000, Manda and Macmillan [2000]). Holocene volcanoes are marked by black triangles.

in 20 km (seismic coupling zone) and 60 km (dehydration processes). This is in contrast with the Central Andes, where the depth-distribution of seismicity is not continuous and the center of intermediate seismicity has been found in 100 km depth. Crustal seismicity is almost exclusively confined to the coastal region, where the forearc is uplifted, presumably due to basal accretion (J. Lohrmann, pers. comm.).

From the refraction experiment, a two-dimensional velocity model was constructed, with low seismic velocities in the sedimentary basins of the Central Valley and the Neuquén basin (2–5.8 km/s), an upper crust of $v_p = 5.9$ –6.3 km/s with from the forearc (15 km) to the volcanic arc decreasing thickness (9 km), and a lower crust with $v_p = 6.8$ –6.9 km/s, which's lower boundary (Moho) increases from 25–30 km beneath the forearc to 35 km below the Main Cordillera. First results from receiver function analysis place the Moho in 40 km depth (X. Yuan, pers. comm.). This compared to the Central Andes moderate crustal thickness manifests itself in a moderate Bouguer anomaly of < 150 mGal.(Z. Tasarova, pers. comm.).